

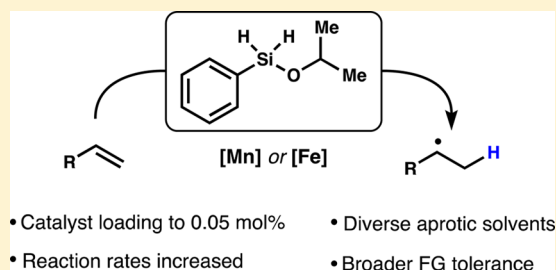
Ph(*i*-PrO)SiH₂: An Exceptional Reductant for Metal-Catalyzed Hydrogen Atom Transfers

Carla Obradors, Ruben M. Martinez, and Ryan A. Shenvi*

Department of Chemistry, The Scripps Research Institute, La Jolla, California 92037, United States

S Supporting Information

ABSTRACT: We report the discovery of an outstanding reductant for metal-catalyzed radical hydrofunctionalization reactions. Observations of unexpected silane solvolysis distributions in the HAT-initiated hydrogenation of alkenes reveal that phenylsilane is not the kinetically preferred reductant in many of these transformations. Instead, isopropoxy(phenyl)silane forms under the reaction conditions, suggesting that alcohols function as important silane ligands to promote the formation of metal hydrides. Study of its reactivity showed that isopropoxy(phenyl)silane is an exceptionally efficient stoichiometric reductant, and it is now possible to significantly decrease catalyst loadings, lower reaction temperatures, broaden functional group tolerance, and use diverse, aprotic solvents in iron- and manganese-catalyzed hydrofunctionalizations. As representative examples, we have improved the yields and rates of alkene reduction, hydration, hydroamination, and conjugate addition. Discovery of this broadly applicable, chemoselective, and solvent-versatile reagent should allow an easier interface with existing radical reactions. Finally, isotope-labeling experiments rule out the alternative hypothesis of hydrogen atom transfer from a redox-active β -diketonate ligand in the HAT step. Instead, initial HAT from a metal hydride to directly generate a carbon-centered radical appears to be the most reasonable hypothesis.



INTRODUCTION

In the 1980s, Mukaiyama reported a powerful method to functionalize electron-neutral alkenes, apparently through radical intermediates.¹ This groundbreaking work enabled the appendage of hydrogen and a functional group to a double bond with Markovnikov selectivity and high chemoselectivity, which subsequently allowed challenging disconnections on complex molecules.

A toolkit of synthetic methods^{2–8} has arisen following the seminal reports of hydration, hydroperoxidation, and hydro-nitrosation of alkenes by cobalt, manganese, and iron complexes (Scheme 1). The intermediate carbon-centered radical or organometallic can react with oxygen in the hydration (1 to 2);^{2a,d,8a–d} with electrophilic fluorine sources in the fluorination;^{4c,8e} with a sulfonate in the chlorination,^{4a,8c} azidation,^{3e} or cyanation;^{6c,8c} with a diazodicarboxylate^{3e} or nitrosoarene^{3k} in the hydroamination; or with a hydrazone in the methylation reaction.^{6h} However, catalyst deactivation frequently occurs after a few turnovers and most of these transformations require an alcoholic solvent that competitively consumes the silane. In some cases, reducible groups such as aldehydes and nitriles react competitively in the presence of alkenes, and superstoichiometric amounts of the silane or high catalyst loadings are required. Most methodologies also allow little variation in the reaction conditions (e.g., lower temperature and concentration or fewer equivalents of the radical trap), which impedes the optimization of low-yielding or excessively slow examples. These restrictions may become problematic for interfacing this direct radical generation method with existing organometallic engines. Our

group has modified the Mukaiyama conditions to achieve stereoselective hydrogenation, reductive cyclization,^{7b} alkene isomerization, diene cycloisomerization, arene annulation, and retro-cycloisomerization.^{6f}

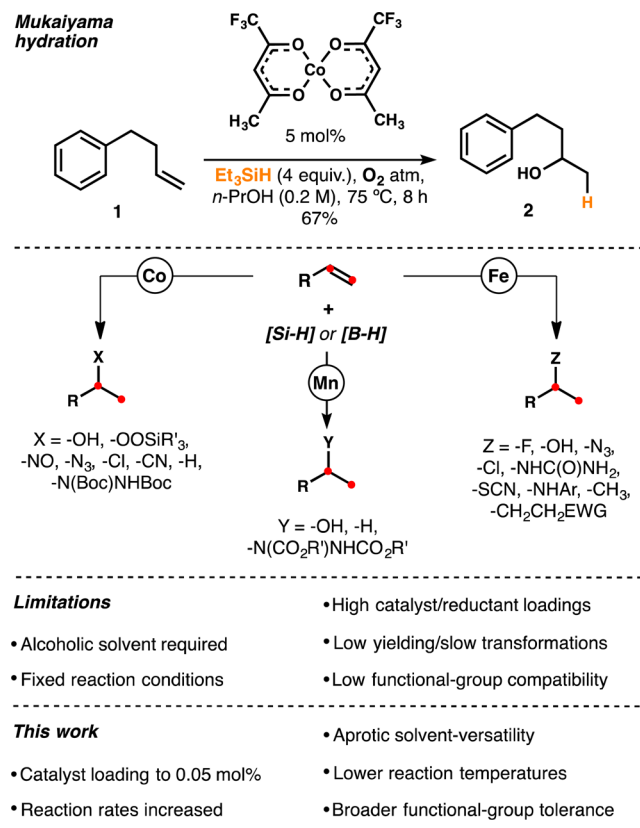
Based on evidence from the literature and our own observations, we proposed these reactions proceed by initial hydrogen atom transfer (HAT) from a metal hydride to directly generate a carbon-centered radical from the alkene. Early precedent for such a mechanism can be found in the stoichiometric HAT hydrogenation of anthracene and styrene with metal hydrides such as HMn(CO)₅. These studies suggested direct and reversible formation of a radical cage pair;⁹ dissociation of this pair was identified as the rate-determining step of the reduction. Similarly, in the context of our stereoselective HAT hydrogenation using PhSiH₃ (3) as a stoichiometric reductant (Scheme 2), manganese catalysts were found to be superior to cobalt catalysts, which may become trapped as off-cycle organometallics via collapse of a carbon-centered radical/metal pair.^{6f,7b,c} As observed previously,^{1,7a} the dipivaloylmethane (dpm) ligand induced higher reaction rates than acetylacetonate (acac) at a modest (10 mol %) catalyst loading for most of the examples.

However, like many previous HAT-initiated reactions mediated by iron and manganese, alcohol was required as solvent. Obviously, this solvent restriction can be problematic for cationic^{2f,3j,10} and anionic^{6a,e,g,11} radical-polar crossover reac-

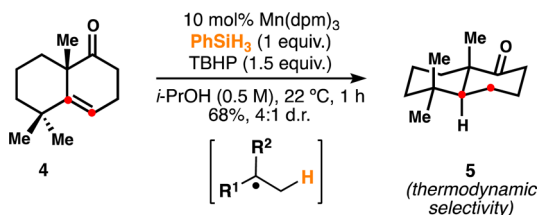
Received: February 23, 2016

Published: March 16, 2016

Scheme 1. Alkene Hydrofunctionalization Toolkit



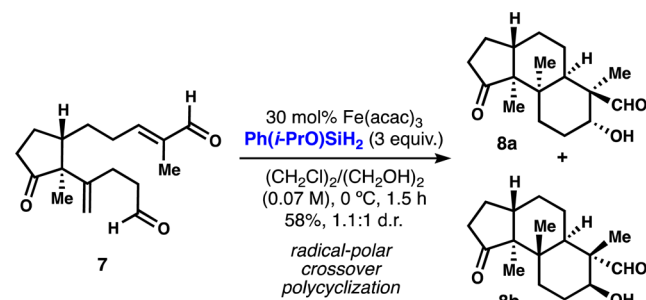
Scheme 2. Stereoselective Hydrogenation of Alkenes



tions, where nucleophilic and protic solvents lead to charge quenching. Here we demonstrate that isopropoxy(phenyl)silane (6, $\text{Ph}(i\text{-PrO})\text{SiH}_2$) is a uniquely efficient reductant that permits the use of multiple solvents in manganese and iron-catalyzed reactions. In most cases, rates of reactions are increased, required reaction temperatures are decreased, and the catalyst loading of our HAT hydrogenation can be dropped as low as 0.05 mol %. Notably, isopropoxy(phenyl)silane increases the efficiency of other reactions within the growing arsenal of HAT-initiated hydrofunctionalizations. The ability to generate carbon-centered radicals from diverse unsaturated building blocks under these chemoselective conditions has led to a rapid growth of the field. Discovery of this broadly applicable, chemoselective, and solvent-versatile reagent should allow an easier interface with existing radical reactions.

For example, we privately disclosed this reagent to the Pronin group who vividly illustrated its potential in a recent synthesis of emindole SB.¹¹ A key step in this work consists of a radical-polar crossover cyclization based on radical conjugate addition followed by intramolecular aldol cyclization (Scheme 3). Reactions of 7 as well as other analogs using phenylsilane produced 8a/8b in low yield and with multiple byproducts, but the reaction was significantly improved by use of $\text{Ph}(i\text{-PrO})\text{SiH}_2$.

Scheme 3. Key Step in the Total Synthesis of Emindole SB



RESULTS AND DISCUSSION

Study of the Intermediates Formed in the HAT Hydrogenation: Discovery of Isopropoxy(phenyl)silane. We had speculated that the alcoholic solvent in HAT-initiated hydrofunctionalization (with Mn and Fe) was necessary only to increase the hydridic character of the silane reductant through formation of a pentavalent silane, as observed by Schowen and others.¹² In our initial experiments, we observed that the HAT hydrogenation in hexanes reduces very little terpeneol (Table 1, entry 1), whereas addition of increasing amounts of isopropanol slowly rescues the reaction (entries 2–4), albeit at 10 mol % $\text{Mn}(\text{dpm})_3$.

Table 1. Increase in Reduction Yield with Increased *i*-PrOH

entry	additive	conversion (%)	yield (%)	d.r.
1	none	35	17	9.5
2	1 equiv of <i>i</i> -PrOH	51	46	7.4
3	2 equiv of <i>i</i> -PrOH	63	57	7.6
4	5 equiv of <i>i</i> -PrOH	82	76	7.7

However, when monitoring consumption of PhSiH_3 by GC, we observed a non-consistent distribution of the silane-derived products: PhSiH_3 was converted to $\text{Ph}(i\text{-PrO})\text{SiH}_2$, $\text{Ph}(i\text{-PrO})_2\text{SiH}$ (11), traces of $\text{PhSi}(\text{O}(i\text{-Pr}))_3$, $(\text{Ph}(i\text{-PrO})_2\text{Si})_2\text{O}$, $\text{Ph}(i\text{-PrO})(t\text{-BuO})\text{SiH}$, and $\text{Ph}(i\text{-PrO})(\text{dpm})\text{SiH}$ among other unidentified species. Interestingly, the first solvolysis product remained at low abundance throughout the reaction (Figure 1). The observation that $\text{Ph}(i\text{-PrO})\text{SiH}_2$ (6) was consumed more rapidly than the other silanes led us to hypothesize that it might

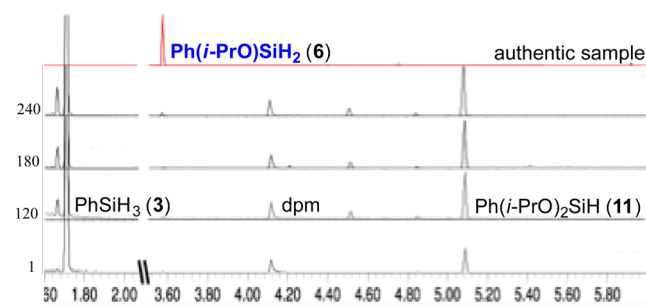
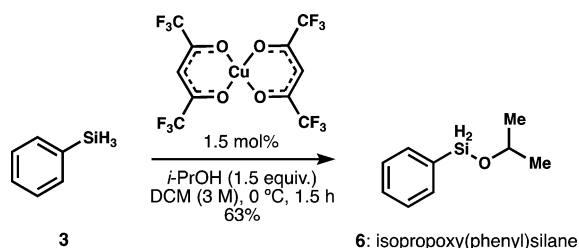


Figure 1. Consumption of phenylsilane (3) in the presence of $\text{Mn}(\text{dpm})_3$, TBHP, and isopropanol from 1 to 240 min.

serve as a superior reductant. Additionally, these data suggested that alcohols do not just act as reaction media or proton sources to turn over the catalyst in radical-anion crossover reactions. Instead, alcohols function as important silane ligands in HAT-initiated reactions, likely as a result of increased Si electrophilicity and more rapid ligand exchange with the catalyst (dpm, isopropoxy, or TBHP).

The available literature revealed limited examples of mono-alkoxysilanes. We prepared isopropoxy(phenyl)silane (**6**) in 30 g scale by adapting the procedure reported by Yamada et al. based on the reaction between phenylsilane and isopropanol in the presence of catalytic copper(II) hexafluoroacetylacetonate ($\text{Cu}(\text{hfac})_2$, Scheme 4).¹³ Unlike other methods, this solvolysis

Scheme 4. Synthesis of Isopropoxy(phenyl)silane



selectively forms (**6**) and only generates diisopropoxy(phenyl)silane (**11**) as a minor byproduct (7%). Manganese, iron, cobalt, nickel, ruthenium, or platinum complexes did not selectively generate monosolvolyzed silanes. Interestingly, attempts to isolate the solvolysis product derived from phenylsilane and ethanol, i.e. ethoxy(phenyl)silane, were not successful due to the moisture sensitivity of this adduct. In contrast, metal-catalyzed solvolysis with *tert*-butanol was sluggish, and therefore the isopropoxy ligand was identified as optimal for investigation. The correspondence of this procedure to the reaction conditions required for most HAT-initiated transformations is clear, which encouraged us in our new hypothesis.

Study of the Reactivity of Isopropoxy(phenyl)silane in the HAT Hydrogenation. Our first generation HAT hydrogenation conditions reduce terpineol **9** in 89% yield with 10 mol % catalyst in isopropanol, but the yield drops precipitously when lowering the catalyst loading or changing solvent (Table 2, entries 1–4).

In contrast, use of $\text{Ph}(i\text{-PrO})\text{SiH}_2$ (**6**) leads to complete consumption of terpineol at 1 mol % catalyst (entries 6 and 8). Moreover, in hexanes at least 2000 turnovers are reached (0.05 mol % Mn, entry 10).¹⁴ We noted that for both silanes the diastereoselectivity of the reaction degraded when the amount of isopropanol was increased, presumably due to the involvement of a larger reductant favoring an equatorial delivery in the second HAT. Interestingly, at lower catalyst loadings higher selectivities were observed. Double solvolysis product diisopropoxy(phenyl)silane (**11**) was less effective in both isopropanol and hexanes (entries 12 and 13).

Reagent **6** tolerates several solvents, including non-anhydrous EtOAc, toluene, acetonitrile, THF, and dichloromethane (Figure 2). The diastereoselectivity for all cases remained in a close range (see Supporting Information (SI) for further details).¹⁵ Otherwise, the reaction with phenylsilane and 10 mol % of $\text{Mn}(\text{dpm})_3$ was generally low yielding even when there was significant consumption of the starting material. The use of DMF as solvent leads to poor yields for both **3** and **6**.

Table 2. Effects of **6** on the Catalyst Loading of the HAT Hydrogenation^a

entry	silane	conditions	conv./yield (%) ^b	d.r.
1	3	<i>i</i> -PrOH, 10 mol %	94/89	7.5
2	3	<i>i</i> -PrOH, 1 mol %	61/53	8.3
3	3	<i>i</i> -PrOH, 0.1 mol %	27/28	9.2
4	3	hexanes, 10 mol %	35/17	9.5
5	6	<i>i</i> -PrOH, 10 mol %	99/98	4.1
6	6	<i>i</i> -PrOH, 1 mol % ^c	100/87	5.5
7	6	hexanes, 10 mol %	94/93	5.2
8	6	hexanes, 1 mol %	100/97	6.3
9	6	hexanes, 0.1 mol %	100/91	6.6
10	6	hexanes, 0.05 mol % ^c	100/98	6.6
11	6	hexanes, 0.02 mol % ^c	48/15	6.2
12	11	<i>i</i> -PrOH, 10 mol %	98/86	5.3
13	11	hexanes, 10 mol %	49/33	5.9

^aReactions performed with 1 equiv of PhSiH_3 , 1.5 equiv of $\text{Ph}(i\text{-PrO})\text{SiH}_2$, or 3 equiv of $\text{Ph}(i\text{-PrO})_2\text{SiH}$. ^bDetermined by GC-FID using 1 equiv of decane as internal standard. ^cReaction time 13 h.

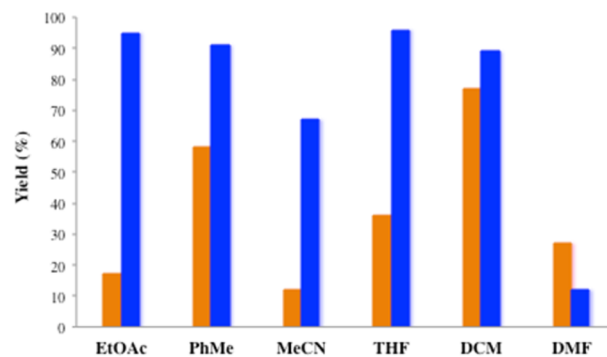
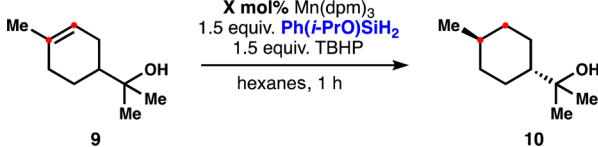


Figure 2. Comparison of the solvent tolerance between silanes **3** (first column, 10 mol %) and **6** (second column, 1 mol %) in the HAT hydrogenation of terpineol.

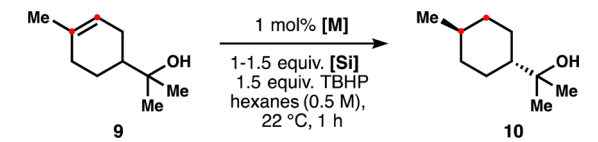
The concentration of the HAT hydrogenation when using isopropoxy(phenyl)silane can be decreased or increased with little effect on the reactivity (Table 3, entries 1–3). Interestingly, the transformation was slower under diluted conditions but led to a slight increase in diastereoselectivity. The reaction can also be run at low temperatures, which progressively increases the d.r. to 11.3 (entries 4–5).¹¹ Fortunately, the 25-fold less-expensive catalyst $\text{Mn}(\text{acac})_3$ (Sigma) performs reasonably well in the reaction with **6**, forming **10** in 89% yield, d.r. 7.2 (Table 4, entry 2), whereas this catalyst performs poorly with PhSiH_3 . Co- and Fe-catalysts are also less effective (3–4). The remainder of the silanes screened were inactive under the optimized reaction conditions (entries 5–9).

Finally, attempts to reduce terpineol in the absence of any silane or any metal complex led to no formation of the desired product **10** (Scheme 5). However, excluding silane from the reaction led to partial consumption of **9** toward an unidentified mixture of products, implying competitive background reactivity in the HAT hydrogenation. Interestingly, 7% of reduction (d.r.

Table 3. Versatility of the Reaction Conditions Using 6 in the HAT Hydrogenation



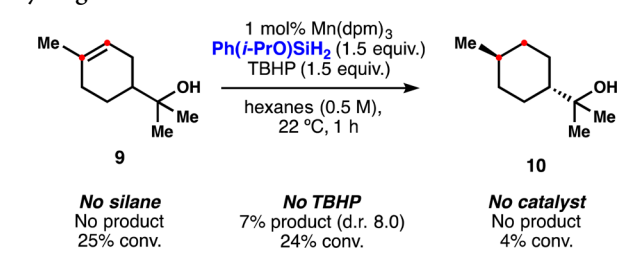
entry	temp (°C)	conditions	conv/yield (%) ^a	d.r.
1	22	0.1 mol %, 1 M	100/92	6.3
2	22	0.1 mol %, 0.25 M	99/97	6.6
3	22	0.1 mol %, 0.1 M ^b	100/97	7.6
4	0	1 mol %, 0.5 M	91/91	7.5
5	-30	1 mol %, 0.5 M	96/71	11.3

^aDetermined by GC-FID using 1 equiv of decane as internal standard.^bReaction time 13 h.Table 4. Reactivity of Alternative Catalyst/Silanes in the HAT Hydrogenation^a


entry	silane	catalyst	conv/yield (%) ^b	d.r.
1 ^c	3	Mn(acac) ₃	31/25	10.5
2	6	Mn(acac) ₃	96/89	7.2
3	6	Fe(dpm) ₃	53/17	5.3
4	6	Co(dpm) ₂	39/35	6.3
5	Ph ₂ SiH ₂	Mn(dpm) ₃	19/0	—
6	Ph ₃ SiH	Mn(dpm) ₃	3/0	—
7	PMHS	Mn(dpm) ₃	26/0	—
8	Et ₃ SiH	Mn(dpm) ₃	32/0	—
9	DEMS	Mn(dpm) ₃	33/3	—

^aReactions performed with 1 equiv of PhSiH₃ or 1.5 equiv for the rest.^bDetermined by GC-FID using 1 equiv of decane as internal standard.^cUse of 10 mol % catalyst in isopropanol.

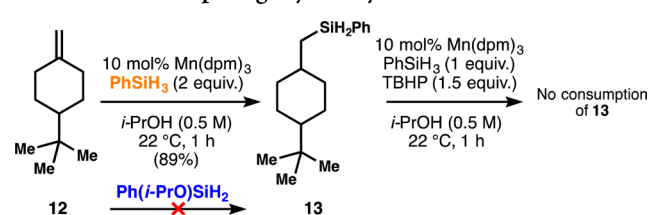
Scheme 5. Study of the Background Reactivity in the HAT Hydrogenation



increased to 8.0) was observed in the absence of TBHP but very rapid catalyst deactivation occurred.

Discovery of a Competing Hydrosilylation Reaction: Different Behaviors between Phenylsilane and Isopropoxy(phenyl)silane. Finally, we also noted that, in the absence of TBHP, certain substrates give rise to a competing, occasionally dominant hydrosilylation pathway using phenylsilane (Scheme 6), probably through addition of a silane radical to the alkene, and radical chain propagation via Si–H abstraction by the tertiary carbon radical.¹⁶ However, we have not found silane 6 to cause hydrosilylation. The industrial importance of

Scheme 6. A Competing Hydrosilylation Reaction



hydrosilylation and the natural abundance of manganese may make this transformation also valuable.

Silane 13 is unreactive under the HAT hydrogenation conditions and is therefore unlikely to be involved in the reduction mechanism. These results suggest multiple roles for TBHP including reoxidation of the metal complex and suppression of competing side reactions. Moreover, TBHP might also be involved in the ligand exchange with the catalyst, which is much more efficient with silane 6 presumably as a result of increased Si electrophilicity.

Kinetic Profiles of the HAT Hydrogenation. As shown in Figure 3, we observed silane 6 to exhibit much higher rates of

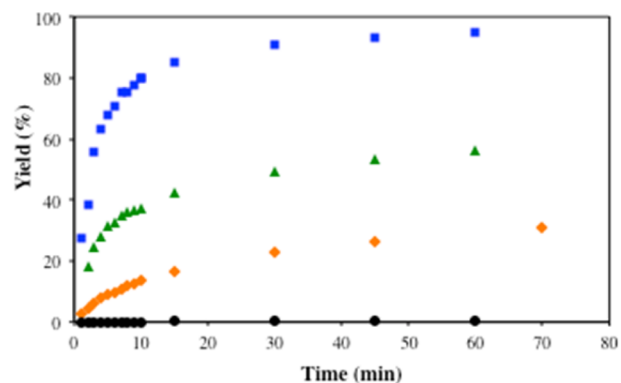


Figure 3. Reduction of terpeneol 9 monitored by GC-FID. Reaction performed with Ph(i-PrO)SiH₂ in hexanes (blue ■) or isopropanol (green ▲) and with PhSiH₃ in hexanes (black ●) or isopropanol (orange ◆).

hydrogenation than PhSiH₃. At 1 mol % catalyst, PhSiH₃ is ineffective in hexanes (0.25 M) for the HAT hydrogenation of terpeneol 9, but its performance in *i*-PrOH is still poor.

Interestingly, the optimum performance of 6 occurs in hexanes, whereas *i*-PrOH decreases the rate, although even here 6 far surpasses 3. We noted that the reduction rates of 9 significantly dropped over time independent of the silane or the solvent used. Conversely, we also observed a variation in the diastereoselectivity, which increased over time in the cases studied. For instance, silane 6 in hexanes led to an increase in d.r. from 5.6 to 6.7 in 60 min, whereas silane 3 in isopropanol gave an increase of 7.0 to 10.1 (see SI for further details). These results suggested a complex mechanistic scenario for the alkene reduction, in which the source of hydrogen may change over time, in line with solvolysis affecting rates of hydrogen transfer.

Study of the Applicability of Isopropoxy(phenyl)silane in the HAT Hydrogenation. These second generation conditions lead to higher yields at lower catalyst, reductant, and oxidant loadings than our first generation conditions for a subset of previously poorly performing alkenes.

In some cases the gains are modest, in others profound, for example, in aldehydes and ketones such as 14 and 15. In our first

generation system, those substrates proved problematic due to competitive reduction,¹⁷ whereas alkenes can be reduced preferentially with **6**—a 929% (3 mol %) and 168% increase (1 mol %), respectively (Figure 4). Aldehyde **14** is highly

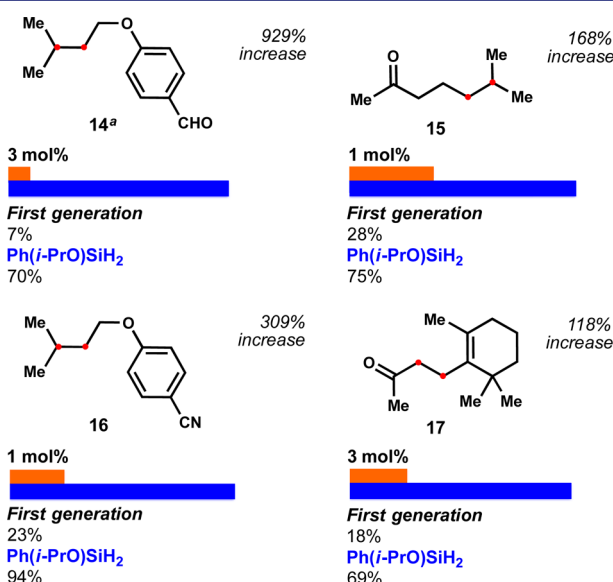


Figure 4. Reduction of alkenes bearing susceptible functional groups. Reactions performed with 1.5 equiv of [Si]/TBHP at 22 °C for 15–60 min. The solvent used was optimized for each substrate with **6**, and isopropanol was required for **3** (see SI for further information). ^aReaction performed at 0 °C.

sensitive under the reaction conditions, and good efficiency was only achieved at 0 °C. Reduction of the alkene of nitrile **16** was also drastically more effective with **6** and 1 mol % of catalyst (309% increase) as well as unsaturated carbonyl **17** (118% increase). All the examples performed with phenylsilane required the use of isopropanol as solvent whereas silane **6** allowed a solvent screen to further increase the yields.

Besides increasing yields, isopropoxy(phenyl)silane obviated the need for a superstoichiometric reductant and oxidant (e.g., 6 equiv of PhSiH₃, 4 equiv of TBHP) or a high catalyst loading (e.g., 20 mol %).^{7b,c} This is the case for enol ether **18** and haloalkenes **19**, **20**, and **21**, which were reduced significantly more efficiently than our first generation conditions (Figure 5). Interestingly, although good yields were obtained for trisubstituted haloalkenes (79% and 70%), an impurity in the reaction tended to inhibit turnover, hampering complete conversion; related protocols required stoichiometric amounts of catalyst for similar scaffolds.^{7c}

Treatment of dienes such as **22** with a silane in the presence of Mn(dpm)₃ leads to the HAT-initiated reductive cyclization (Scheme 7).^{7b} In this example, the metal hydride generates a carbon-centered radical that is engaged by a pendant alkene to form a subsequent radical that is reduced. The cyclization step competitively forms the five- and six-membered rings independent of the silane or solvent used in the reaction (**23a** and **23b**, respectively). This intrinsic behavior is consistent with a radical transformation.¹⁵ With 1 mol % of catalyst the first-generation conditions lead to the reductive cyclization in 28% isolated yield whereas isopropoxy(phenyl)silane increases this yield to 87%.

Styrenes continue to be poorly performing substrates (Figure 6), although even **24** improved with **6** (styrenes tend to dimerize

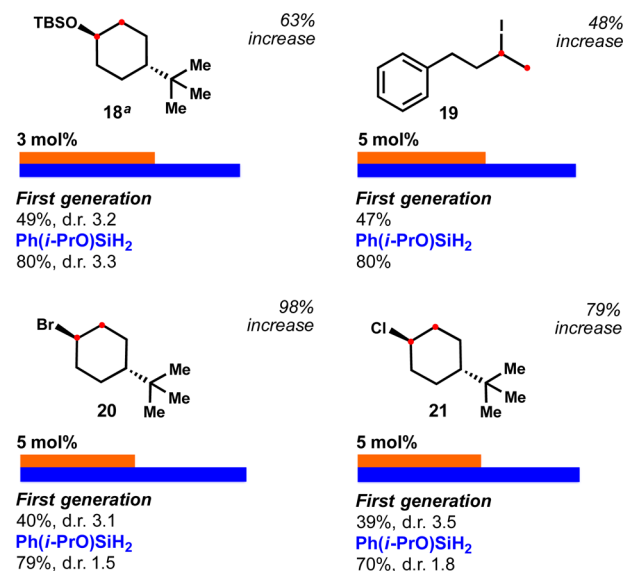


Figure 5. Reduction of enol ethers and haloalkenes. Reactions performed with 2 equiv of [Si]/TBHP at 22 °C for 4 h. The solvent used was optimized for each substrate with **6**, and isopropanol was required for **3** (see SI for further information). ^aAddition of 1 equiv of CaCO₃.

Scheme 7. Comparison between Silanes **3** and **6** in the HAT-Initiated Reductive Cyclization

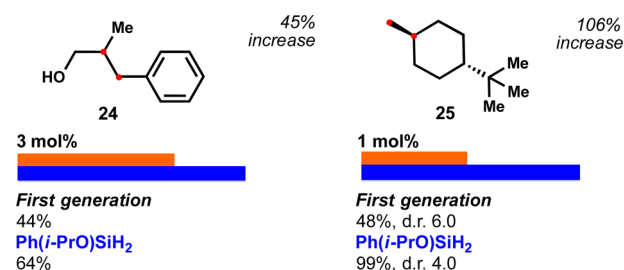
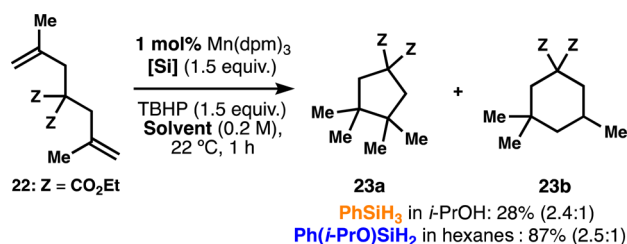


Figure 6. Comparison of the reduction of a styrene and an exocyclic alkene with silane **3** and **6** (see SI for further information).

through a persistent benzyl radical, which could be minimized by performing the reduction under more dilute conditions). *tert*-Butyl-methylenecyclohexane **25** on the other hand is reduced quantitatively with **6** in only 15 min, but rather inefficiently with **3**.

Hydrogenation of hindered Δ^{5,6} steroids such as cholesterol (**26**) can be modestly improved with **6** (Figure 7). An important, if esoteric, showcase example for the continuing utility of the generally thermodynamic preference of alkene reduction is shown in example **27**. Here a Δ^{4,5} steroid is reduced to the *trans*-A/B ring junction (confirmed by X-ray crystallography, Figure 8),¹⁸ whereas all literature precedent shows, to the best of our knowledge, preference for *cis*- upon catalytic hydrogenation

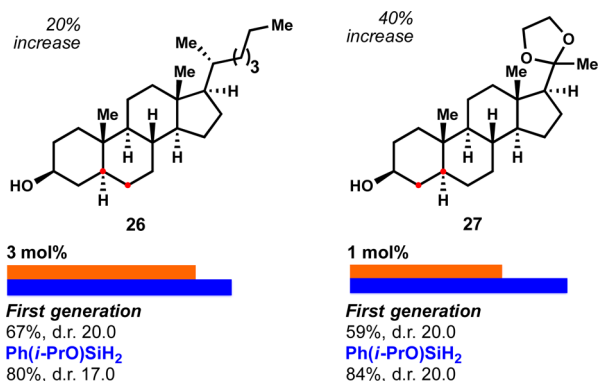


Figure 7. Reduction of hindered alkenes in steroid derivatives. Reactions performed with 2 equiv of $[\text{Si}]/\text{TBHP}$ at 22 °C for 0.5–2 h. The solvent used was optimized for each substrate with **6**, and isopropanol was required for **3** (see SI for further information).

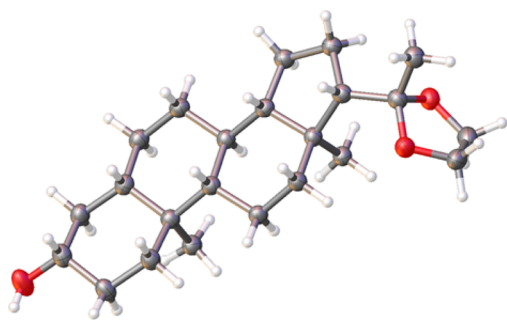


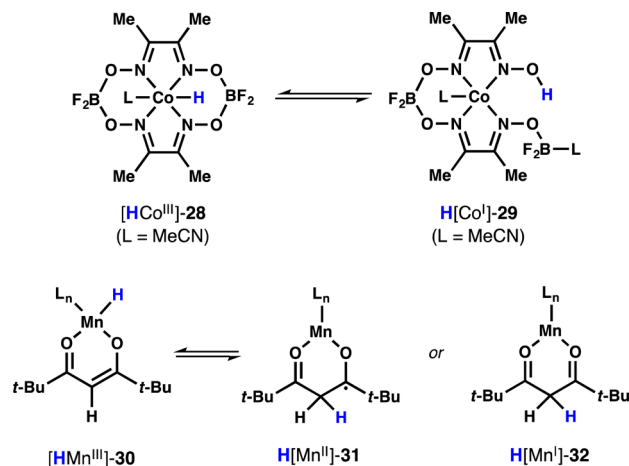
Figure 8. *Trans*-A/B ring junction of **27** confirmed by X-ray crystallography.

(with the exception of dissolving metal reduction, as discussed previously).^{7b}

Isotope Labeling Experiments of the HAT Hydrogenation. As a mechanistic aid to the eventual design of an asymmetric variant of HAT hydrogenation, we sought to identify the source of the second hydrogen addition, which in most cases forms the sole stereogenic center from a prochiral alkene.¹⁹ Many prior studies have examined the source of the first hydrogen using deuterium labeling.^{2e,f,3e,4a,6b,g,d,7a,8a–c,e} Only Herzon has explored double radical hydrogen incorporation under Mukaiyama-type conditions,^{4d} and these studies did not identify the second source of hydrogen incorporation.²⁰ Furthermore, a significant question arose only recently in studies by Norton who demonstrated that $\text{Co}(\text{dmgBF}_2)_2\text{-H}$ complexes **28** and **29** may exist as equilibria of Co-H and O-H tautomers, either of which could undergo HAT (Scheme 8).²¹ We wondered whether hydrogen in our Mn-catalyzed system could derive from a non-innocent ligand and hydrogen scrambling between a metal center and its ligand could occur. The analogous structure for metal hydride β -diketonate **30** would involve C–H tautomer **31** or **32**. Since silane **6** gave us the ability to hydrogenate alkenes in aprotic solvent that cannot exchange with free or bound diketonate, we interrogated these competing sources of hydrogen/deuterium.

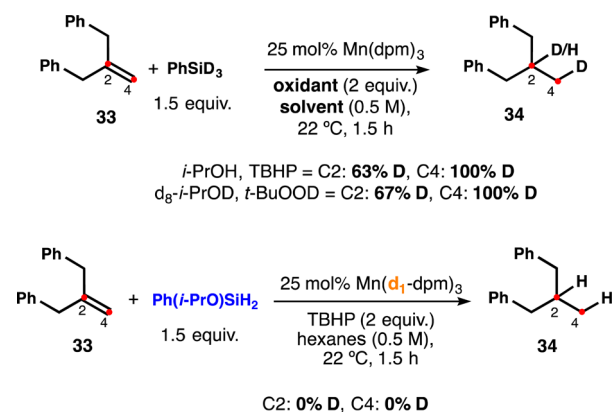
Hydrogenation of substrate **33** with PhSiD_3 and $\text{Mn}(\text{dpm})_3$ showed complete incorporation at C4 (100%, i.e. 66% H integration by ^1H NMR). These results are consistent with repeated observations of complete initial (C4) deuterium incorporation²² using PhSiD_3 or NaBD_4 and a non-deuterated ligand.^{2e,f,3e,4a,6b,g,d,7a,8a–c,e} However, these prior data alone do not exclude hydrogen scrambling with the ligand due to the

Scheme 8. Tautomerization of Metal Complexes



inverse kinetic isotope effect associated with metal hydride HAT; i.e., the Mn–D might be preferentially transferred to the alkene even as a small population in equilibrium.²³ Moreover, only 63% D was observed at C2, suggesting a competing non-silane-derived source for the second hydrogen (Scheme 9). However,

Scheme 9. Involvement of the Ligand in the Hydrogen Atom Transfer

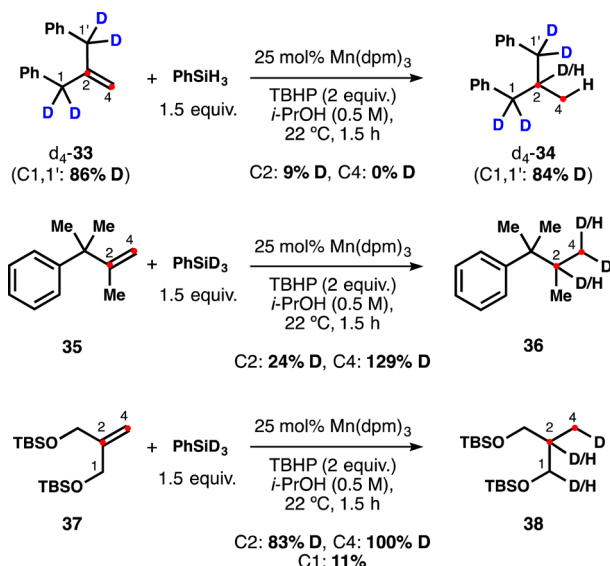


deuterated catalyst $\text{Mn}(d_1\text{-dpm})_3$ (25 mol %) in hexanes leads to no deuterium incorporation at either C2 or C4. The absence of deuteration could not be due to a high $k_{\text{H}}/k_{\text{D}}$ via C–H HAT²⁴ in light of the previous PhSiD_3 incorporation experiments. Based on these data, there is no evidence that HAT results from a redox-active (C–H bond forming) non-innocent β -diketonate ligand.

When the hydrogenation was performed in *d*₈-*i*-PrOD or using *t*-BuOOD, we observed no D incorporation at either C2 or C4,^{7c} despite the low bond dissociation energy of hydroperoxy O–H bonds, ruling out these alternative sources of H or D (see SI for further details). But more surprisingly, hydrogenation of **33** with PhSiD_3 and *t*-BuOOD in *d*₈-*i*-PrOD led to very similar results, i.e. only partial deuteration at the internal carbon C2. We observed that reduction of **33** under more dilute conditions led to very little improvement (0.1 M, 66% D at C2), with similar results when using an excess of PhSiD_3 (6 equiv, 72% D) or modified catalyst loading (5 mol % Mn, 49% D; and 100 mol % Mn, 68% D). Where was the internal hydrogen coming from?

Deuteration of substrate **33** in the benzylic positions gave us a clue. Reduction of *d*₄-**33** with PhSiH_3 delivered 9% deuterium incorporation at C2 during the hydrogenation (Scheme 10),

Scheme 10. Isotope Scrambling Depending on the Substrate



indicating that the mysterious internal hydrogen is derived from the substrate itself. This level of deuterium incorporation is lower than the reverse isotope labeling (37% H, Scheme 9) likely reflecting a normal KIE of hydrogen transfer. This isomerization could either be mediated by a Mn(II) reverse HAT or intersubstrate transfer. Unless there is a very high inverse KIE from the metal hydride, this scrambling must occur between the intermediate substrate radical and substrate 33, since we see 100% D incorporation at C4 (Scheme 9) and a metal hydride formed by reverse HAT would label C4 with H. Abstraction of the benzylic hydrogen from 33 would not be surprising, since its BDE should lie somewhere between diphenylmethane (81.4 kcal/mol) and 1,4-pentadiene (76.4 kcal/mol), similar to the BDE of 1,4-cyclohexadiene (76.9 kcal/mol), used previously as a stoichiometric reductant.²⁵

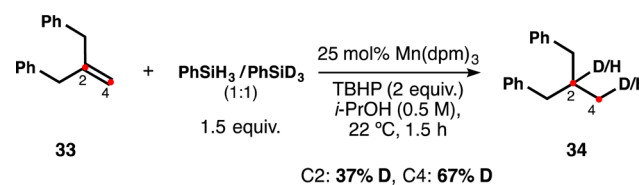
Reduction of substrates 35 and 37 with PhSiD_3 neatly showed 100% deuterium incorporation at C4, but 76% and 17% of hydrogen, respectively, were present at C2. Incorporation of additional deuterium (129% D) at C4 of 36 confirms the equilibrium intermediacy of an alkene subsequent to the initial HAT. Substrate 37, in which the C–H bonds adjacent to the newly formed radical possess higher BDEs than the benzylic positions of 33, demonstrates much lower levels of scrambling, i.e. higher levels of deuterium incorporation. Therefore, the amount of competitive isomerization is highly dependent on the structure of the substrate, and is not intrinsic to all reductions.

Finally, we also observed that the hydrogenation of 33 produced 70% of 34 in the absence of TBHP when 1 equiv of the manganese complex was used. This result suggests that the reduction of the radical intermediate does not occur exclusively from the metal hydride since the Mn(II) product cannot reform a Mn(III)–H (see Scheme 5). Based on this stoichiometric reaction and on the labeling results mentioned above, the main second reductant appears to be the silane itself. The resulting silyl radical can add to alkenes in the absence of TBHP to effect hydrosilylation (see Scheme 6). In the context of hydrogenation, the fate of the resulting silyl radical in the catalytic cycle or alternate radical chain is uncertain—it might form a silylmanganese(III) reservoir—but TBHP appears to play a role in its consumption to prevent hydrosilylation.²⁶ These data also illustrate obstacles to the design of an asymmetric variant of

HAT hydrogenation using the Mukaiyama reaction manifold, especially since a metal complex may only be partially involved in the stereogenic second hydrogen donation.

An intermolecular competition experiment between PhSiH_3 and PhSiD_3 (1:1) in the reduction of 33 revealed major incorporation of deuterium in the terminal C4 position (Scheme 11), whereas no preference was observed in C2 after considering

Scheme 11. H/D Intermolecular Competition Experiment



the background source of hydrogen (isomerization). This preference for D-incorporation demonstrates an inverse KIE present in the catalytic cycle, either at the initial HAT step or in the formation of the metal hydride/deuteride from the metal(III) precatalyst.²⁷

Similarly, comparison of a kinetic profile of PhSiD_3 against PhSiH_3 in the hydrogenation of terpineol 9 in isopropanol showed a small inverse kinetic isotope effect on the overall rate (Figure 9). Such inverse KIEs have been suggested as hallmarks

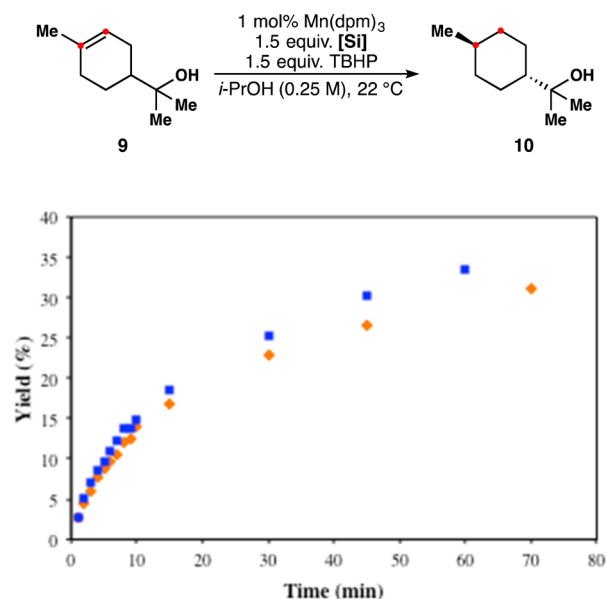


Figure 9. Reduction of terpineol monitored by GC-FID. Reaction performed in isopropanol with PhSiH_3 (orange \blacklozenge) or PhSiD_3 (blue \blacksquare).

of an HAT mechanism in stoichiometric reductions mediated by metal hydrides.⁹ The relatively small size of the observed KIE may suggest a tempering effect of normal KIEs at other points in the catalytic cycle, but we are cautious to overinterpret this observation, since precatalyst formation might also lead to an inverse KIE. Nevertheless, this is the first inverse KIE observed in the Mukaiyama literature and establishes an important point of departure for subsequent mechanistic study.²⁸

Combined with work from our lab showing that organocobalt complexes appear to be parasitic species in HAT isomerization,^{6f} and that AIBN or alcohol^{2a} can replace silane reductant using cobalt catalysis, these results support the hypothesis that these

hydrofunctionalizations proceed by metal hydride HAT to an alkene and exclude the competing alternatives of hydro-metalation and ligand HAT. Obviously, reductive elimination pathways are not available to the planar tetradentate porphyrin or salen metal complexes frequently used in this chemistry.²⁹ Given the high energy of carbon-centered radicals and the low bond dissociation enthalpy of C–H bonds adjacent to carbon radicals, these M–H HAT reactions must rely on the surprisingly high reactivity of the intermediate metal hydrides.⁹

Study of the Applicability of Isopropoxy(phenyl)silane in Other HAT-Initiated Hydrofunctionalizations: Hydration of Alkenes. In his seminal publications, Mukaiyama reported the hydration of alkenes using a silane in an alcoholic solvent in the presence of a cobalt complex and oxygen (1 atm). Later, Magnus reported the use of manganese catalysts³⁰ in the umpolung hydration of α,β -unsaturated compounds.^{2d} Silane 6 increases the performance of Mn-catalyzed hydration of **1** in a non-alcoholic solvent (Figure 10). The reaction affords **2** using 5

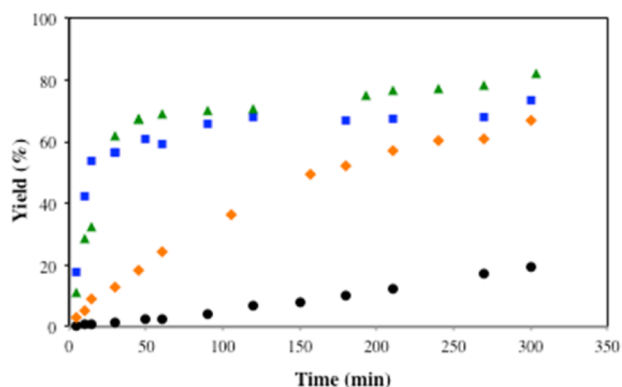
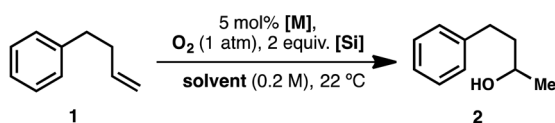


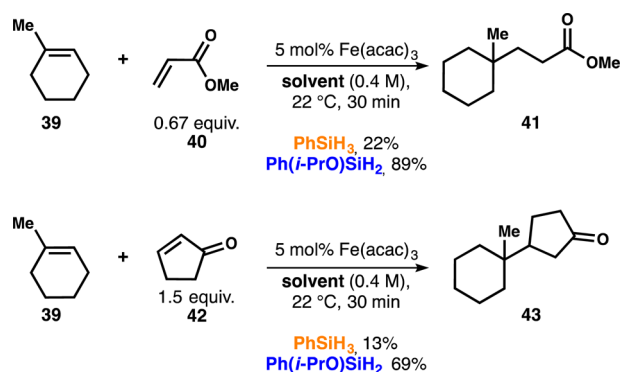
Figure 10. Hydration of phenylbutene **1** with O_2 monitored by GC-FID. Reaction performed with $Mn(acac)_3/Ph(i-PrO)SiH_2$ in THF (green \blacktriangle), $Mn(dpm)_3/Ph(i-PrO)SiH_2$ in THF (blue \blacksquare) and $Mn(acac)_3/PhSiH_3$ in THF (black \bullet) or isopropanol (orange \blacklozenge). $Co(acac)_2/PhSiH_3$ and $Ph(i-PrO)SiH_2$ in THF are both efficient.

mol % of either $Mn(dpm)_3$ or $Mn(acac)_3$ in THF under O_2 atmosphere, but $PhSiH_3$ performs poorly in the absence of isopropanol. Interestingly, $Co(acac)_2$ was a competent catalyst with both **3** and **6** in THF.

Study of the Reductive Olefin Coupling. In addition to improving the yields, catalyst loadings, and solvent breadth of HAT hydrogenation, isopropoxy(phenyl)silane (**6**) allows Baran's iron-catalyzed conjugate addition to be run at low catalyst loadings and ambient temperature.^{6c} As shown in Scheme 12, $PhSiH_3$ (**3**) does not perform well towards the formation of **41** or **43** under those conditions.

In contrast, silane **6** significantly outstrips silane **3** and gives yields comparable to, or better than, the original conditions, which used high catalyst loading and excess of enone or alkene (30–40 mol % $[Fe]$, 3 equiv of **39** or **42**, EtOH, 60 °C). Interestingly, no turnover was observed in the absence of an alcoholic solvent also with silane **6**; isopropanol was used as a cosolvent of EtOAc or DCM, as a proton source is

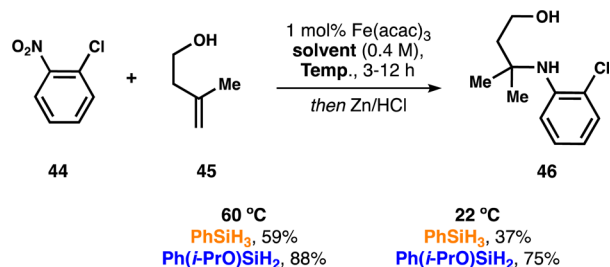
Scheme 12. Comparison of Silane **3** and **6** in the Radical Conjugate Addition



mechanistically required for this transformation. Thus, the radical intermediate attacks the α,β -unsaturated carbonyl, which presumably forms an iron enolate that becomes protonated to afford the final product and reoxidize the catalyst.

Study of the Hydroamination of Alkenes. Similarly, silane **6** allows the recently reported HAT-initiated iron-catalyzed hydroamination of alkenes to be run using a low catalyst loading (1 mol %) and ambient temperature (Scheme 13).^{3k}

Scheme 13. Comparison of Silane **3** and **6** in the Hydroamination of Alkenes



The reaction leads from good to excellent yields, whereas the efficiency was highly reduced with $PhSiH_3$ in isopropanol. In this case, the results suggested that the radical intermediate attacked a nitroso group that would be subsequently reduced and protonated; therefore, a minimum of 3 equiv of an alcohol were also required for the formation of **46** (see SI for further details).

CONCLUSIONS

We have shown that the required alcohol solvent used in Mn- and Fe-catalyzed HAT-initiated hydrofunctionalizations partly serves as an accelerating substituent on the silane reductant. This solvent restriction posed a significant limitation to the field, which hampered the refinement of the established protocols, as we have shown here. The intermediate reductant derived from isopropanol, $Ph(i-PrO)SiH_2$ (**6**), greatly improves many of these reactions, including our first generation HAT hydrogenation, hydration, and hydroamination of alkenes as well as the reductive olefin coupling. Isopropoxy(phenyl)silane can accelerate and improve HAT-mediated transformations that are non-optimal under standard conditions. Outstanding results have been obtained: decreased catalyst loadings down to 0.05 mol %, lowered reaction temperatures, and use of diverse, aprotic solvents, which preclude superstoichiometric amounts of

reagents, and broader functional group tolerance. The solvent versatility also allowed novel radical-polar crossover methods, as the Pronin group has already shown in a recent synthesis of emindole SB.¹¹ We also include data to suggest that HAT does not occur from the ligand, which is an alternative hypothesis for HAT reactions involving the dimethylglyoxime (dmg) ligand. Further isotope labeling experiments revealed preferential deuterium incorporation during the HAT along with hydrogen scrambling from the substrate. Moreover, discovery of a competing hydrosilylation reaction revealed multiple roles for TBHP besides reoxidation of the catalyst. The mechanistic hypothesis that currently best fits the data is M-H HAT to the alkene forming a carbon-centered radical. Thus, the structural and energetic implications from this HAT hypothesis, along with the versatility provided by Ph(*i*-PrO)SiH₂, should stimulate many discoveries and facilitate the invention of new chemical reactions. New methods and applications in chemical synthesis are currently under development in our group.

■ ASSOCIATED CONTENT

● Supporting Information

The Supporting Information is available free of charge on the ACS Publications website at DOI: 10.1021/jacs.6b02032.

Crystallographic data (CIF)

Detailed experimental procedures, spectral data and chromatograms (PDF)

■ AUTHOR INFORMATION

Corresponding Author

*rshenvi@scripps.edu

Present Address

Department of Chemistry, The Scripps Research Institute, 10550 North Torrey Pines Road, La Jolla, California 92037, United States

Notes

The authors declare no competing financial interest.

■ ACKNOWLEDGMENTS

Financial support for this work was provided by the NIH (GM104180 and F31 GM111050 to R.M.). Additional support was generously provided by Eli Lilly, Novartis, Bristol-Myers Squibb, Amgen, Boehringer-Ingelheim, the Sloan Foundation, and the Baxter Foundation. We thank Dr. Curtis Moore and Prof. Arnold L. Rheingold for X-ray crystallographic analysis. We thank Professor Dale Boger for valuable discussions.

■ REFERENCES

- (1) For a review and references to early work, see: (a) Mukaiyama, T.; Yamada, T. *Bull. Chem. Soc. Jpn.* **1995**, *68*, 17. (b) Hoffmann, R. W. *Chem. Soc. Rev.* **2016**, *45*, 577.
- (2) C–O bond formation: (a) Mukaiyama, T.; Isayama, S.; Inoki, S.; Kato, K.; Yamada, T.; Takai, T. *Chem. Lett.* **1989**, *18*, 449. (b) Isayama, S.; Mukaiyama, T. *Chem. Lett.* **1989**, *18*, 573. (c) Isayama, S.; Mukaiyama, T. *Chem. Lett.* **1989**, *18*, 1071. (d) Magnus, P.; Payne, A. H.; Waring, M. J.; Scott, D. A.; Lynch, V. *Tetrahedron Lett.* **2000**, *41*, 9725. (e) Tokuyasu, T.; Kunikawa, S.; McCullough, K. J.; Masuyama, A.; Nojima, M. *J. Org. Chem.* **2005**, *70*, 251. (f) Shigehisa, H.; Aoki, T.; Yamaguchi, S.; Shimizu, N.; Hiroya, K. *J. Am. Chem. Soc.* **2013**, *135*, 10306. (g) Hu, X.; Maimone, T. J. *J. Am. Chem. Soc.* **2014**, *136*, 5287.
- (3) C–N bond formation: (a) Kato, K.; Mukaiyama, T. *Chem. Lett.* **1990**, *19*, 1395. (b) Kato, K.; Mukaiyama, T. *Chem. Lett.* **1990**, *19*, 1917. (c) Hata, E.; Kato, K.; Yamada, T.; Mukaiyama, T. *J. Synth. Org. Chem. Jpn.* **1996**, *54*, 728. (d) Gaspar, B.; Waser, J.; Carreira, E. M. *Synthesis*

- 2007**, 3839. (e) Waser, J.; Gaspar, B.; Nambu, H.; Carreira, E. M. *J. Am. Chem. Soc.* **2006**, *128*, 11693. (f) Waser, J.; González-Gómez, J. C.; Nambu, H.; Huber, P.; Carreira, E. M. *Org. Lett.* **2005**, *7*, 4249. (g) Waser, J.; Nambu, H.; Carreira, E. M. *J. Am. Chem. Soc.* **2005**, *127*, 8294. (h) Waser, J.; Carreira, E. M. *Angew. Chem., Int. Ed.* **2004**, *43*, 4099. (i) Waser, J.; Carreira, E. M. *J. Am. Chem. Soc.* **2004**, *126*, 5676. (j) Shigehisa, H.; Koseki, N.; Shimizu, N.; Fujisawa, M.; Niitsu, M.; Hiroya, K. *J. Am. Chem. Soc.* **2014**, *136*, 13534. (k) Gui, J.; Pan, C.-M.; Jin, Y.; Qin, T.; Lo, J. C.; Lee, B. J.; Spengel, S. H.; Mertzman, M. E.; Pitts, W. J.; La Cruz, T. E.; Schmidt, M. A.; Darvatkar, N.; Natarajan, S. R.; Baran, P. S. *Science* **2015**, *348*, 886.

- (4) C–X (halide) bond formation: (a) Gaspar, B.; Carreira, E. M. *Angew. Chem., Int. Ed.* **2008**, *47*, 5758. (b) Gaspar, B.; Waser, J.; Carreira, E. M. *Org. Synth.* **2010**, *87*, 88. (c) Shigehisa, H.; Nishi, E.; Fujisawa, M.; Hiroya, K. *Org. Lett.* **2013**, *15*, 5158. (d) Ma, X.; Herzon, S. B. *Chem. Sci.* **2015**, *6*, 6250.

- (5) C–S/Se bond formation: (a) Girijavallabhan, V.; Alvarez, C.; Njoroge, F. G. *J. Org. Chem.* **2011**, *76*, 6442. (b) Reference 4d.

- (6) C–C bond formation: (a) Isayama, S.; Mukaiyama, T. *Chem. Lett.* **1989**, *18*, 2005. (b) Wang, L.-C.; Jang, H.-Y.; Roh, Y.; Lynch, V.; Schultz, A. J.; Wang, X.; Krische, M. J. *J. Am. Chem. Soc.* **2002**, *124*, 9448. (c) Gaspar, B.; Carreira, E. M. *Angew. Chem., Int. Ed.* **2007**, *46*, 4519. (d) Gaspar, B.; Carreira, E. M. *J. Am. Chem. Soc.* **2009**, *131*, 13214. (e) Lo, J. C.; Yabe, Y.; Baran, P. S. *J. Am. Chem. Soc.* **2014**, *136*, 1304. (f) Crossley, S. W. M.; Barabé, F.; Shenvi, R. A. *J. Am. Chem. Soc.* **2014**, *136*, 16788. (g) Lo, J. C.; Gui, J.; Yabe, Y.; Pan, C.-M.; Baran, P. S. *Nature* **2014**, *516*, 343. (h) Dao, H. T.; Li, C.; Michaudel, Q.; Maxwell, B. D.; Baran, P. S. *J. Am. Chem. Soc.* **2015**, *137*, 8046. (i) Zheng, J.; Wang, D.; Cui, S. *Org. Lett.* **2015**, *17*, 4572.

- (7) C=C reduction: (a) Magnus, P.; Waring, M. J.; Scott, D. A. *Tetrahedron Lett.* **2000**, *41*, 9731. (b) Iwasaki, K.; Wan, K. K.; Oppedisano, A.; Crossley, S. W. M.; Shenvi, R. A. *J. Am. Chem. Soc.* **2014**, *136*, 1300. (c) King, S. M.; Ma, X.; Herzon, S. B. *J. Am. Chem. Soc.* **2014**, *136*, 6884. (d) Reference 4d.

- (8) For a related set of radical hydrofunctionalizations, discovered independent of references 1–7 and based on iron complexes/borohydrides, see: (a) Ishikawa, H.; Colby, D. A.; Boger, D. L. *J. Am. Chem. Soc.* **2008**, *130*, 420. (b) Ishikawa, H.; Colby, D. A.; Seto, S.; Va, P.; Tam, A.; Kakei, H.; Rayl, T. J.; Hwang, I.; Boger, D. L. *J. Am. Chem. Soc.* **2009**, *131*, 4904. (c) Leggans, E. K.; Barker, T. J.; Duncan, K. K.; Boger, D. L. *Org. Lett.* **2012**, *14*, 1428. (d) Gotoh, H.; Sears, J. E.; Eschenmoser, A.; Boger, D. L. *J. Am. Chem. Soc.* **2012**, *134*, 13240. (e) Barker, T. J.; Boger, D. L. *J. Am. Chem. Soc.* **2012**, *134*, 13588.

- (9) (a) Feder, H. M.; Halpern, J. *J. Am. Chem. Soc.* **1975**, *97*, 7186. (b) Sweany, R. L.; Halpern, J. *J. Am. Chem. Soc.* **1977**, *99*, 8335. (c) Eisenberg, D. C.; Norton, J. R. *Isr. J. Chem.* **1991**, *31*, 55. (d) Choi, J.; Tang, L.; Norton, J. R. *J. Am. Chem. Soc.* **2007**, *129*, 234.

- (10) (a) Abley, P.; Dockal, E. R.; Halpern, J. *J. Am. Chem. Soc.* **1972**, *94*, 659. (b) Magnuson, R. H.; Halpern, J.; Levitin, I. Y.; Vol'pin, M. E. *J. Chem. Soc., Chem. Commun.* **1978**, 44.

- (11) George, D. T.; Kuenstner, E. J.; Pronin, S. V. *J. Am. Chem. Soc.* **2015**, *137*, 15410.

- (12) (a) O'Donnell, K.; Bacon, R.; Chellappa, K. L.; Schowen, R. L.; Lee, J. K. *J. Am. Chem. Soc.* **1972**, *94*, 2500. (b) Howie, C. R.; Lee, J. K.; Schowen, R. L. *J. Am. Chem. Soc.* **1973**, *95*, 5286. (c) Revunova, K.; Nikonov, G. I. *Chem. Eur. J.* **2014**, *20*, 839.

- (13) Gunji, Y.; Yamashita, Y.; Ikeno, T.; Yamada, T. *Chem. Lett.* **2006**, *35*, 714.

- (14) The stark drop in conversion between entries 10 and 11 probably indicates inhibition from an impurity near 0.0002 equiv abundance. However, neither the impurity nor its source could be identified.

- (15) Beckwith, A. L. J.; Bowry, V. W.; Ingold, K. U. *J. Am. Chem. Soc.* **1992**, *114*, 4983.

- (16) (a) Chatgililoglu, C. *Acc. Chem. Res.* **1992**, *25*, 188. (b) Chen, C.; Hecht, M. B.; Kavara, A.; Brennessel, W. W.; Mercado, B. Q.; Weix, D. J.; Holland, P. L. *J. Am. Chem. Soc.* **2015**, *137*, 13244.

- (17) (a) Magnus, P.; Fielding, M. R. *Tetrahedron Lett.* **2001**, *42*, 6633. (b) Yamada, T.; Ikeno, T.; Ohtsuka, Y.; Kezuka, S.; Sato, M.; Iwakura, I. *Sci. Technol. Adv. Mater.* **2006**, *7*, 184 and references cited therein.

(18) CCDC 1445790 contains the supplementary crystallographic data for this paper (27 X-ray). These data are provided free of charge by the Cambridge Crystallographic Data Centre.

(19) Sibi, M. P.; Porter, N. A. *Acc. Chem. Res.* **1999**, *32*, 163.

(20) In ref 8b, treatment of anhydrovinblastine with superstoichiometric amounts of $\text{Fe}_2(\text{ox})_3$ and NaBD_4 in the absence of oxygen led to alkene reduction with complete deuterium incorporation in both carbons, suggesting differences in the reaction paths between this and our work.

(21) Estes, D. P.; Grills, D. C.; Norton, J. R. *J. Am. Chem. Soc.* **2014**, *136*, 17362.

(22) In ref 7c, partial deuterium incorporation is observed, but many sources of hydrogen are present.

(23) Anslyn, E. V.; Dougherty, D. A. *Modern Physical Organic Chemistry*; University Science Books: 2006.

(24) Mayer, J. M. *Acc. Chem. Res.* **2011**, *44*, 36.

(25) (a) Cherkasov, A.; Jonsson, M. *J. Chem. Inf. Comput. Sci.* **2000**, *40*, 1222. (b) Pratt, D. A.; Mills, J. H.; Porter, N. A. *J. Am. Chem. Soc.* **2003**, *125*, 5801. (c) Gao, Y.; DeYonker, N. J.; Garrett, E. C., III; Wilson, A. K.; Cundari, T. R.; Marshall, P. J. *Phys. Chem. A* **2009**, *113*, 6955.

(26) Chatgililoglu, C. *Chem. Rev.* **1995**, *95*, 1229.

(27) Simmons, E. M.; Hartwig, J. F. *Angew. Chem., Int. Ed.* **2012**, *51*, 3066.

(28) In ref 3e, the cobalt(III)-catalyzed hydrohydrazination and hydroazidation of olefins showed normal kinetic isotope effects (2.2 and 1.65, respectively), demonstrating differences in rate-determining steps between these and the hydrogenation reactions.

(29) (a) Gridnev, A. A.; Ittel, S. D. *Chem. Rev.* **2001**, *101*, 3611. (b) De Bruin, B.; Dzik, W. L.; Li, S.; Wayland, B. B. *Chem. Eur. J.* **2009**, *15*, 4312. (c) Sorokin, A. B. *Chem. Rev.* **2013**, *113*, 8152.

(30) Inoki, S.; Kato, K.; Isayama, S.; Mukaiyama, T. *Chem. Lett.* **1990**, 1869.